Journal of the European Ceramic Society **19** (1999) 907–912
© 1999 Elsevier Science Limited
Printed in Great Britain. All rights reserved
PII: S0955-2219(98)00342-2
0955-2219/99/$ - see front matter

Processing and Characterisation of Fine Crystalline Ceria Gadolinia–Yttria Stabilized Zirconia Powders

A. Tsoga,* A. Naoumidis, W. Jungen and D. Stöver

Institute for Materials and Processes in Energy Systems, IWV1, Research Center Jülich, D-52425 Jülich, Germany

Abstract

For low temperature SOFCs the yttria stabilized zirconia (YSZ)-coated ceria is a promising candidate for replacing YSZ-electrolyte. An important requirement for the co-firing feasibility of such a configuration is the densification of ceria at low temperatures (< 1400°C). Fine crystalline gadolinia doped ceria (CGO)-powder readily sinterable at 1250°C was synthesized by co-precipitation with oxalic acid of 0·05 M and crystallization in methanol at 200°C for 6 h. The fabrication and characterisation of solid solution phases with a graded composition $(CGO)_x(YSZ)_{1-x}$*, to be used as an interlayer between YSZ and CGO, in order to avoid delamination, were also studied and discussed.* CGO_xYSZ_{1-x} *powders, prepared by the glycine combustion method, required higher sintering temperatures (1500°C) to densify, while they showed significantly lower ionic conductivity than YSZ and CGO, attributed to the large lattice deformation and scattering of oxygen ions. © 1999 Elsevier Science Limited. All rights reserved*

Keywords: YSZ, powders: chemical preparation, sintering, fuel cells.

1 Introduction

Ceria electrolytes have recently received much interest as possible candidate substitutes for solid oxide fuel cell (SOFC) applications, as an alternative to the established YSZ electrolyte. As compared to zirconia the use of a ceria-based electrolyte presents the advantages of superior ionic conductivity and compatibility with more active electrodes such as lanthanum cobaltites, allowing in this way the reduction of the operating temperature of the cell. This decrease in operating temperature means both a cost reduction, since the use of low-cost metallic components as separator materials is then possible, and a prolonged stack lifetime.

The problems associated with the use of ceria-based electrolytes are mainly related to the high reducibility of ceria in the fuel-gas environment, its poor sinterability and the lack of large-scale fabrication methods for industrial applications.[1,2] For doped ceria to become at least as attractive as YSZ, these problems must be addressed. As concerns the reducibility, it has been already demonstrated that it can be addressed for example by a coating of YSZ at the reducing side, which blocks the electronic leak current.[3,4] However the co-firing of such a ceria/YSZ double layer thin film electrolyte configuration still suffers from serious solid-state reaction and diffusion phenomena between YSZ and ceria, mainly taking place above 1400°C, and delaminating of the composite film.[5]

To avoid extended interdiffusion phenomena between YSZ and CGO the possibility to synthesise CGO-powder readily sinterable at temperatures lower than 1400°C was examined. Solid solution phases with a graded composition $(CGO)_x(YSZ)_{1-x}$, to be possibly used as an interlayer between YSZ and CGO, in order to produce non-laminated composite films were fabricated and characterised.

2 Experimental

The different chemical routes investigated concerned: the urea–nitrate combustion method which directly produces a crystalline powder, due to the high temperature during urea combustion (≈1200°C), the spray-drying method and two strike co-precipitation methods using ammonia or oxalic acid as precipitants. As best technique for

---

*To whom correspondence should be addressed. Fax: +49-2461-61-5700; e-mail: a.tsoga@fz-juelich.de the synthesis of $(CeO_2)_{0\cdot 8}(GdO_{1\cdot 5})_{0\cdot 2}$ was found to be the strike co-precipitation with oxalic acid. $Ce^{III}(NO_3)_3.6H_2O$ (>98·5% Merck) and Gd_2O_3 (99·9% Fluka) dissolved in HNO_3 (65%, $d=1\cdot 4$ Merck) were used as starting materials, dissolved in the correct stoichiometric proportion in a minimum amount of distilled water. The nitrate solution was then added dropwise to a thoroughly stirred oxalic acid solution with an excess of 2 in $C_2O_4^{2-}$ concentration. The resulting amorphous precipitate was vacuum filtered, washed three times with ethanol to remove water and dried. Optimisation of the selected technique was carried out considering the influence of different parameters, such as washing agent, precipitant concentration and crystallisation process, on the powder properties (Table 1).

For the preparation of $(CGO)_x(YSZ)_{1-x}$ solid solutions phases, two kinds of strike co-precipitation methods were investigated with ammonium oxalate or ammonium hydroxide as precipitants and the glycine–nitrate combustion technique. Based on powder composition and sintered bodies density results, the technique adopted was glycine-nitrate combustion. The starting materials for Ce and Gd were the same as before, while for Zr and Y we used $ZrO(NO_3)_2.xH_2O$ (Fluka, 25·8 wt% in Zr) and $Y(NO_3)_3.6H_2O$ (>99% Merck), respectively. A precursor was prepared by combining glycine H_2NCH_2COOH (Merck 99·7%) with metal nitrates in their appropriate stoichiometric ratios in aqueous solution. The precursor was dried overnight at 100°C to evaporate excess water, yielding a viscous liquid. Further heating on a hot plate maintained at 180°C caused the precursor liquid to auto-ignite, with a flame (1100–1450°C), yielding a foamy, fine, crystalline powder. Calcination of the powders at 400°C removes any possible glycine residues.

The dried gels and crystallised powders were characterised with simultaneous thermal gravimetry and differential thermal analysis (TG-DTA). Compositions were evaluated by an inductively coupled plasma (ICP-OES). Further, the crystallised powders were examined by both scanning electron microscopy and X-ray powder diffractometry (XRD) to evaluate the particle size,

Table 1. Preparation conditions of co-precipitated CGO powders

Point	*Oxalic acid concentration (M)*	*Washing agent*	*Crystallisation conditions*	*Calcination temperature (°C)*	*Crystalline size (nm)*
1	0·5	H_2O	Air, 700°C, 1 h	—	25
2	0·5	EtOH	Air, 700°C, 1 h	—	13
3	0·5	EtOH	MeOH, 200°C, 6 h	400	5
4	0·5	EtOH	MeOH, 200°C, 6 h	650	23
5	0·5	EtOH	MeOH, 200°C, 6 h	900	105
6	0·05	EtOH	MeOH, 200°C, 6 h	650	19
7	0·05	EtOH	MeOH, 200°C, 6 h	900	75

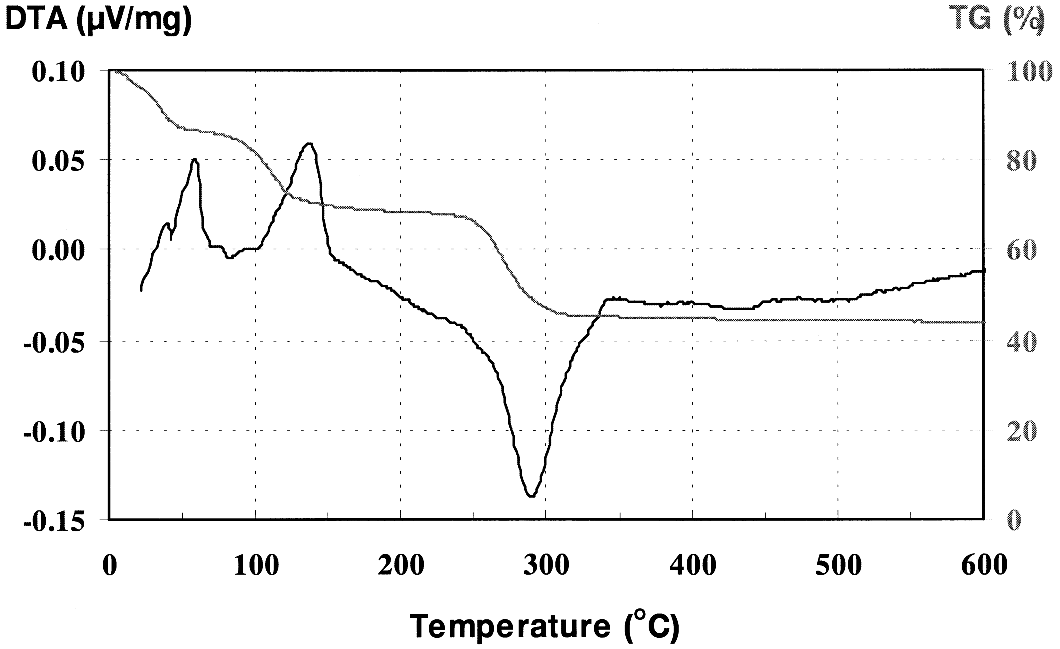

Fig. 1. Differential thermogravimetric analysis of the decomposition of the CGO-powder prepared by thermolysis of the gadolinium-doped cerium oxalate.

crystallite size and the extent of agglomeration in the powders as well as for phase identification and measurements of the lattice parameters. Compacts ($\varnothing = 10\,\mathrm{mm}$) for sintering studies were prepared by uniaxially pressing at 20 MPa. Sintering was carried out in air on YSZ setters with a heating rate of $3°\mathrm{C\,min}^{-1}$ and a holding time of 8 h at each sintering temperature. The bulk density of the sintered bodies was determined by Archimedes' technique and expressed as relative to the theoretical values determined by the XRD cubic lattice parameters. Total conductivity measurements were carried out in air using the dc four-point DC technique.

3 Results and Discussion

3.1 $(CeO_2)_{0{\cdot}8}(GdO_{1{\cdot}5})_{0{\cdot}2}$ powders

The decomposition of the dried gels in air as monitored by thermogravimetric analysis is shown in Fig. 1. The weight loss observed at room temperature up to 150°C with two endothermic peaks refers to organic and water removal, while the oxalate is completely decomposed to the corresponding mixed oxide (exothermic process) between 250 and 350°C. The temperature of the decomposition indicates that the mixed oxalates behave as a solid solution and not as the sum of single oxalates.[6]

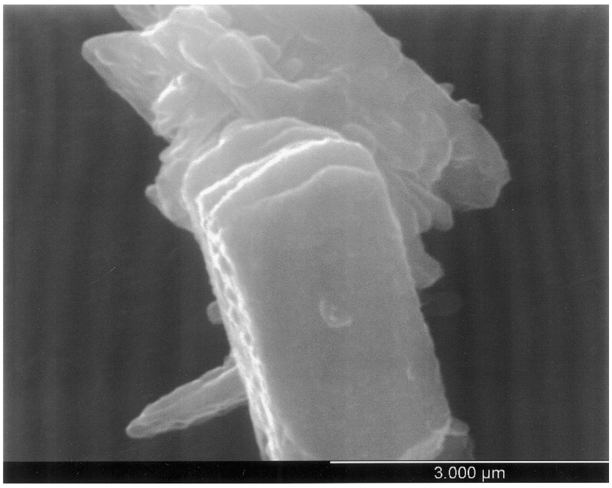

Fig. 2. Agglomerate morphology of the CGO powder prepared by thermolysis of the gadolinium-doped cerium oxalate.

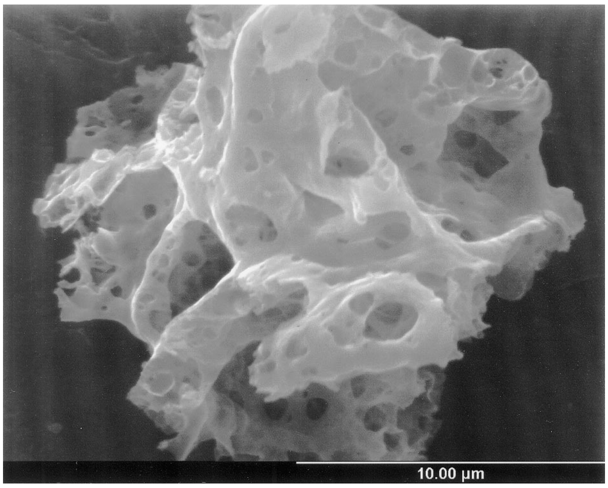

Fig. 4. Typical agglomerate morphology of the CGO_xYSZ_{1-x} powder prepared by the glycine combustion method.

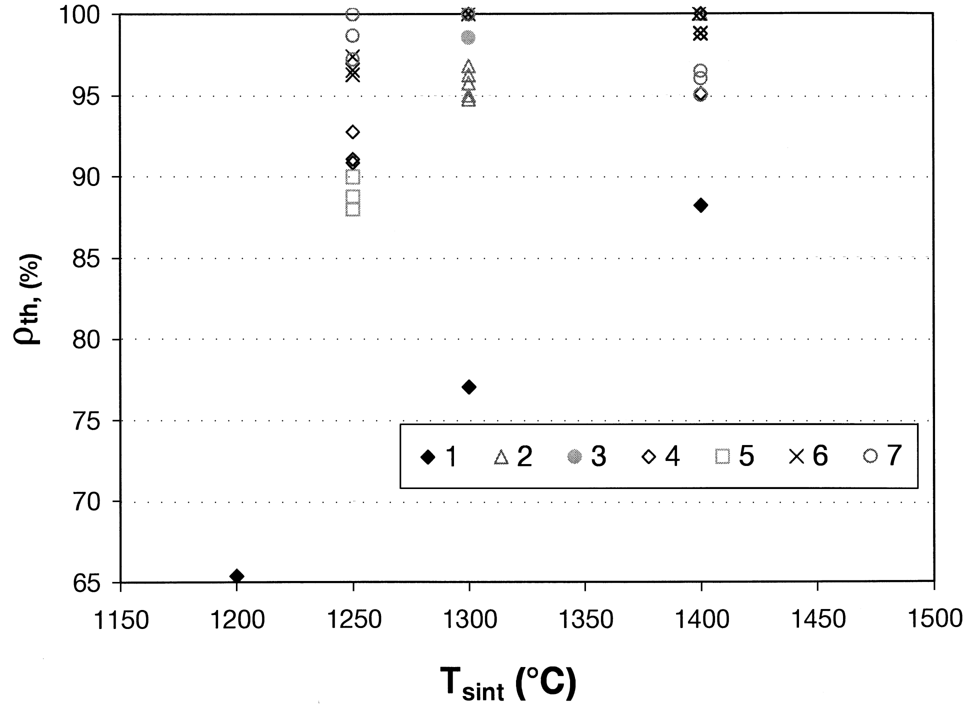

Fig. 3. Relative densities of sintered CGO compacts prepared by co-precipitation with oxalic acid under the conditions described in Table 1.

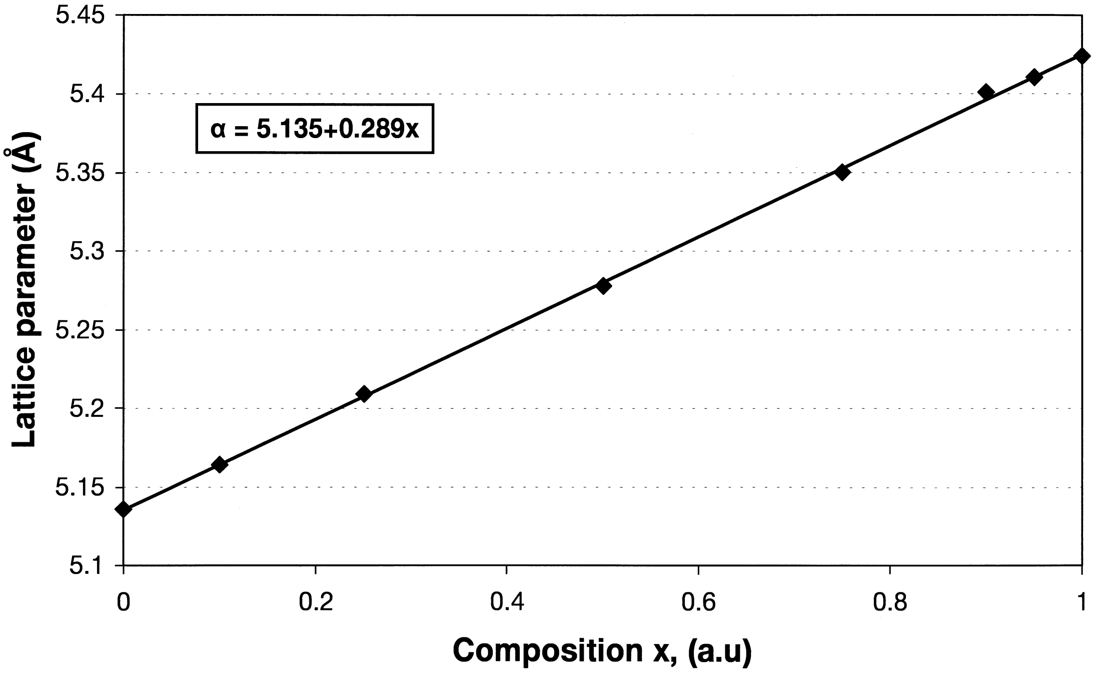

Fig. 5. Variation of lattice parameter (α) with composition x in the $\mathrm{CGO}_x\mathrm{YSZ}_{1-x}$ system.

Table 2. Chemical compositions of the CGO and $\mathrm{CGO}_x\mathrm{YSZ}_{1-x}$ powders (the theoretically calculated values are shown in parentheses)

Composition	*%wt Ce*	*%wt Gd*	*%wt Zr*	*%wt Y*
$\mathrm{CGO}_{0\cdot1}\mathrm{YSZ}_{0\cdot95}$	7·5 (8·3)	2 (2·3)	50·6 (55·7)	10·2 (9·5)
$\mathrm{CGO}_{0\cdot25}\mathrm{YSZ}_{0\cdot75}$	19·3 (19·7)	5·1 (5·5)	43 (44·3)	8·9 (7·6)
$\mathrm{CGO}_{0\cdot5}\mathrm{YSZ}_{0\cdot5}$	34·3 (36·7)	9·5 (10·3)	26·3 (27·5)	4·2 (4·7)
$\mathrm{CGO}_{0\cdot75}\mathrm{YSZ}_{0\cdot25}$	48·5 (51·5)	13·6 (14·4)	12·4 (12·8)	2·0 (2·2)
$\mathrm{CGO}_{0\cdot9}\mathrm{YSZ}_{0\cdot1}$	55·0 (59·4)	15·7 (16·7)	5·0 (4·9)	0·8 (0·8)
$\mathrm{CGO}_{0\cdot95}\mathrm{YSZ}_{0\cdot05}$	60·3 (61·9)	17·1 (17·9)	2·6 (2·4)	0·4 (0·4)
CGO	63·2 (63·8)	17·2 (17·9)	—	—

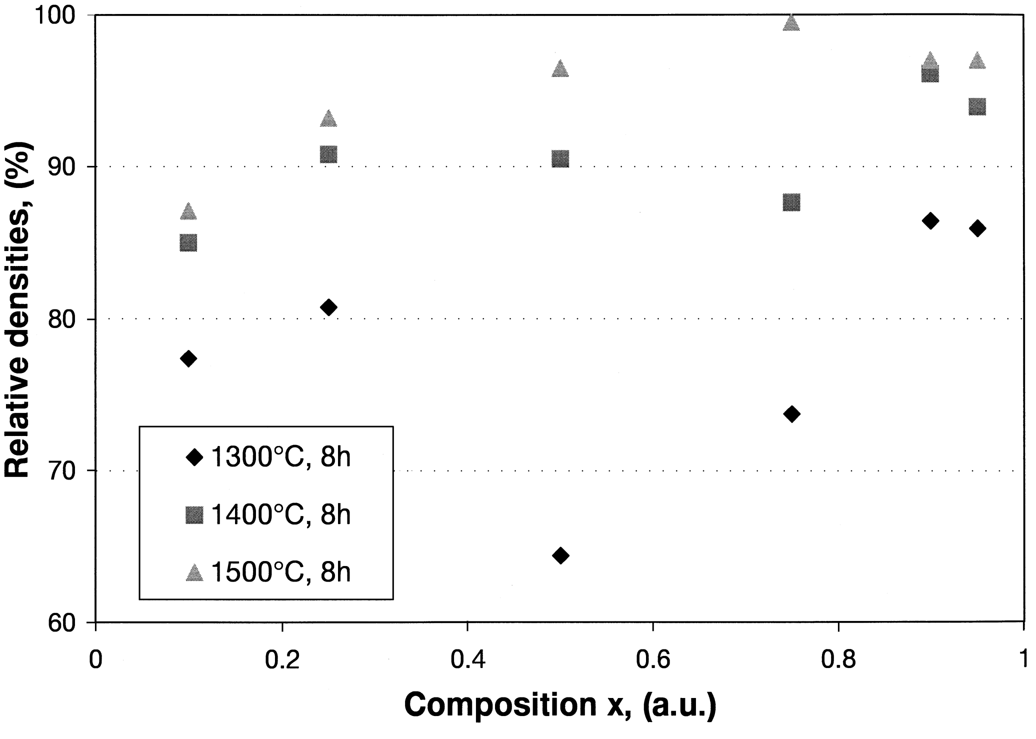

Fig. 6. Variation of the relative densities of the $\mathrm{CGO}_x\mathrm{YSZ}_{1-x}$ compacts with composition x and temperature.

As verified by X-ray diffraction measurements the powder exhibits the cubic fluorite structure with a lattice parameter of 5·4242 Å, being in very good agreement with literature values 5·4312[7] and 5·417 Å,[8] as well as with a theoretically determined value 5·4247 Å, calculated by introducing the concept of the oxygen vacancy radius.[9] The composition of the samples was found to be 62·5 wt% Ce and 17·4 wt% Gd which, compared to the theoretically calculated values, is in between the error limit of the technique used (±2–3%).

Even without milling, the powders obtained showed average submicron particle sizes between 0·3 and 0·8 μm. A reason for this superiority could be the fact that during thermolysis the oxalates decompose into oxides with the simultaneous liberation of a double volume of carbon dioxide, which prevents particles from enhanced agglomeration. The agglomerates were shown to have a plate shape (Fig. 2) which was found to promote sinterability of the powder. Based on density measurements of sintered bodies (Fig. 3) the need for dilute oxalic acid for co-precipitation was identified as one of the most important factors. The dewatering of the precipitate through ethanol, in order to prevent bond formation between adjacent particles and thus the formation of ‘hard’ agglomerates,[10] was also found to be significant. The

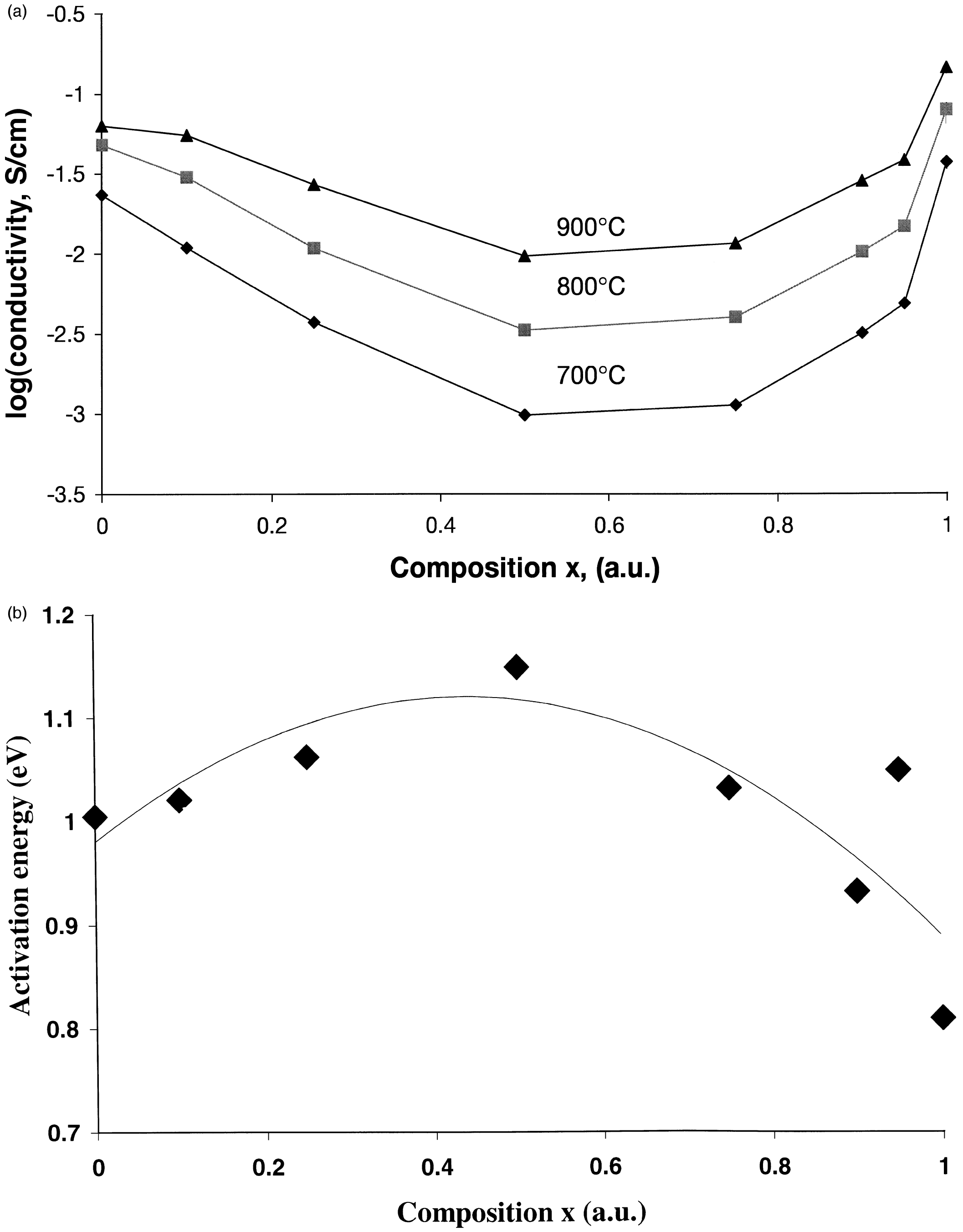

Fig. 7. (a) Variation of logσ with composition x and temperature for the solid solutions CGO_xYSZ_{1-x}; (b) variation of activation energy with composition x for the solid solutions CGO_xYSZ_{1-x}.

formation of 'soft' agglomerates was found to be also favoured by crystallisation in methanol, permitting the compacts to fully densify at temperatures even 150°C lower than that required for the powders crystallised in air (Fig. 3).

3.2 $(CGO)_x(YSZ)_{1-x}$ powders

As verified by SEM and X-ray analysis of the CGO_xYSZ_{1-x} powders, the glycine–nitrate combustion process yields foamy crystalline oxide powders (Fig. 4) with single cubic structure for the whole composition range. The crystalline size of the powders varied between 5 and 15 nm depending on composition. With increasing CGO content (x) the lattice parameters increased linearly (Fig. 5) indicating the formation of a compositionally homogeneous solid solution. The compositions of the solid solution phases prepared, summarised in Table 2, compare well with the theoretically expected values.

Figure 6 shows the relative densities of powder compacts as a function of sintering temperature and composition. Depending on composition, relative densities higher than 95% were attainable for sintering temperatures higher than 1500°C.

Total conductivity values measured in air dependent on composition are shown in Fig. 7(a) for temperatures of 700, 800 and 900°C. Conductivity first decreases with x reaching a minimum at $x = 0{\cdot}5$ and then increases again to reach the conductivity of CGO. This behaviour holds for all three temperatures measured and follows the same trend as that of the CeO_2–YSZ system reported by Ananthapadmanabhan *et al.*[11] On the other hand the variation of the activation energy follows a reverse trend [Fig. 7(b)]. Both conductivity and activation energy variation with composition indicates that the formation of a solid solution between CGO and YSZ restrains the mobility of the oxygen ions, probably due to scattering of oxygen ions, resulting from the large lattice deformation.[11] This effect restricts the use of a CGO_xYSZ_{1-x} solid solution as an interlayer between YSZ and CGO in order to avoid delamination of the single layers. An alternative candidate could be a solid solution between ceria and zirconia with a lower concentration of the trivalent cations (Gd and Y), which still remains to be investigated in future work.

4 Conclusions

1. Fine crystalline CGO-powder, prepared by co-precipitation with oxalic acid and crystallised in methanol at 200°C was sintered to >95% of the theoretical density at 1250°C.
2. Higher sintering temperatures (1500°C) were required for the CGO_xYSZ_{1-x} powders, prepared by the glycine combustion method. Their low ionic conductivity however restricts their use as an interlayer between YSZ and CGO, to avoid delamination of the single layers.
3. The variation of conductivity with composition for the CGO_xYSZ_{1-x} systems was attributed to large lattice deformation and scattering of oxygen ions.

Acknowledgements

The work was carried out in the framework of a Marie-Curie Fellowship TMR Project No. ERB4001GT963909. A. Tsoga is a TMR grant holder. The authors thank P. Lersch for the XRD-measurements.

References

1. Van Herle, J., Horita, T., Kawada, T., Sakai, N., Yokokawa, H. and Dokiya, M., Fabrication and sintering of fine yttria-doped ceria powder. *J. Am. Ceram. Soc.*, 1997, **80**, 933–940.
2. Yahiro, H., Eguchi, K. and Arai, H., Electrical properties and reducibilities of ceria-rare earth oxide systems and their applications to solid oxide fuel cells. *Solid State Ionics*, 1989, **36**, 71–75.
3. Yahiro, H., Baba, Y., Eguchi, K. and Arai, H., High temperature fuel cell with ceria–yttria solid electrolyte. *J. Electrochem. Soc.*, 1988, **135**, 2077–2080.
4. Mehta, K., Hong, S. J., Jue, J. F. and Virkar, A. V., Fabrication and characterisation of YSZ-coated ceria electrolytes. In *Proceedings of the 3rd International Symposium on Solid Oxide Fuel Cells*, Vol. 1(2) ed. S. C. Singhal and H. Iwahara. The Electrochemical Society, 1993, pp. 92–103.
5. Horita, T., Sakai, N., Yokokawa, H., Dokiya, M., Kawada, T., Van Herle, J. and Sasaki, K., Ceria–zirconia composite electrolyte for solid oxide fuel cells. *J. of Electroceramics*, 1997, **1**(2), 155–164.
6. Overs, A. and Riess, I., Properties of the solid electrolyte gadolinia-doped ceria prepared by thermal decomposition of mixed cerium–gadolinium oxalate, *J. Am. Ceram. Soc.*, 1982, **65**, 606–609.
7. Gödickermeier, M., Mixed ionic electronic conductors for solid oxide fuel cells. Ph.D. thesis, Swiss Federal Institute of Technology, Zürich, 1996.
8. Sammes, N. M. and Cai, Z., Ionic conductivity of ceria/yttria stabilised zirconia electrolyte materials. *Solid State Ionics*, 1997, **100**, 39–44.
9. Hong, S. J. and Virkar, A. V., Lattice parameters and densities of rare-earth oxide doped ceria electrolytes. *J. Am. Ceram. Soc.*, 1995, **78**, 433–439.
10. Kaliszewski, M. S. and Heuer, A. H., Alcohol interaction with zirconia powders. *J. Am. Ceram. Soc.*, 1990, **73**, 1504–509.
11. Ananthapadmanabhan, P. V., Venkatramani, N., Rohatgi, V. K., Momin, A. C. and Venkateswarlu, K. S., Structure and ionic conductivity of solid solutions in the system $0{\cdot}9\{8ZrO_2)_{1-x}$–$(CeO_2)_x\}$–$0{\cdot}1(Y_2O_3)$. *J. Europ. Ceram. Soc.*, 1990, **6**, 111–117.